⌘ *Author's Choice*

THE JOURNAL OF BIOLOGICAL CHEMISTRY VOL. 287, NO. 33, pp. 28169–28179, August 10, 2012

GQ-16, a Novel Peroxisome Proliferator-activated Receptor γ (PPARγ) Ligand, Promotes Insulin Sensitization without Weight Gain[S]

Received for publication, December 14, 2011, and in revised form, May 11, 2012 Published, JBC Papers in Press, May 14, 2012, DOI 10.1074/jbc.M111.332106

Angélica A. Amato[a1,2], Senapathy Rajagopalan[b1], Jean Z. Lin[c], Bruno M. Carvalho[d], Ana C. M. Figueira[e3], Jenny Lu[b], Stephen D. Ayers[b], Melina Mottin[f], Rodrigo L. Silveira[f4], Paulo C. T. Souza[f5], Rosa H. V. Mourão[g], Mário J. A. Saad[d], Marie Togashi[a2], Luiz A. Simeoni[a2], Dulcinéia S. P. Abdalla[h], Munir S. Skaf[f], Igor Polikparpov[i], Maria C. A. Lima[j], Suely L. Galdino[j], Richard G. Brennan[k], John D. Baxter[b], Ivan R. Pitta[j], Paul Webb[b], Kevin J. Phillips[b1,6], and Francisco A. R. Neves[a1,2,7]

From the [a]Laboratório de Farmacologia Molecular, Departamento de Ciências Farmacêuticas, Faculdade de Ciências da Saúde, Universidade de Brasília, 70919-970 Brazil, the [b]Diabetes Research Center, Methodist Hospital Research Institute, Houston, Texas 77030, the [c]Department of Biology and Biochemistry, Center for Nuclear Receptors and Cell Signaling, University of Houston, Houston, TX 77204, the [d]Departamento de Medicina Interna, Universidade Estadual de Campinas, Campinas, São Paulo 13083-887, Brazil, the [e]National Institute of Biosciences, Brazilian Association for Synchrotron Light Technology, Campinas, São Paulo 13083-970, Brazil, the [f]Institute of Chemistry, University of Campinas, Campinas, São Paulo 13084-862, Brazil, the [h]Faculdade de Ciências Farmacêuticas, Departamento de Análises Clínicas e Toxicológicas, Universidade de São Paulo, São Paulo, SP 05508-900, Brazil, the [g]Laboratório de Bioprospecção e Biologia Experimental, Universidade Federal do Oeste do Pará, Santarém, Para 68040-070, Brazil, the [j]Departamento de Antibióticos, Universidade Federal de Pernambuco, Recife, Pernambuco 50670-901, Brazil, the [i]Instituto de Física de São Carlos, Departamento de Física e Universidade de São Paulo, SP 13560–970, São Carlos, Brazil, and the [k]Department of Biochemistry, Duke University School of Medicine, Durham, North Carolina 27710, USA

Background: PPARγ agonists improve insulin sensitivity but also evoke weight gain.
Results: GQ-16 is a PPARγ partial agonist that blocks receptor phosphorylation by Cdk5 and improves insulin sensitivity in diabetic mice in the absence of weight gain.
Conclusion: The unique binding mode of GQ-16 appears to be responsible for the compound's advantageous pharmacological profile.
Significance: Similar compounds could have promise as anti-diabetic therapeutics.

The recent discovery that peroxisome proliferator-activated receptor γ (PPARγ) targeted anti-diabetic drugs function by inhibiting Cdk5-mediated phosphorylation of the receptor has provided a new viewpoint to evaluate and perhaps develop improved insulin-sensitizing agents. Herein we report the development of a novel thiazolidinedione that retains similar anti-diabetic efficacy as rosiglitazone in mice yet does not elicit weight gain or edema, common side effects associated with full PPARγ activation. Further characterization of this compound shows GQ-16 to be an effective inhibitor of Cdk5-mediated phosphorylation of PPARγ. The structure of GQ-16 bound to PPARγ demonstrates that the compound utilizes a binding mode distinct from other reported PPARγ ligands, although it does share some structural features with other partial agonists, such as MRL-24 and PA-082, that have similarly been reported to dissociate insulin sensitization from weight gain. Hydrogen/deuterium exchange studies reveal that GQ-16 strongly stabilizes the β-sheet region of the receptor, presumably explaining the compound's efficacy in inhibiting Cdk5-mediated phosphorylation of Ser-273. Molecular dynamics simulations suggest that the partial agonist activity of GQ-16 results from the compound's weak ability to stabilize helix 12 in its active conformation. Our results suggest that the emerging model, whereby "ideal" PPARγ-based therapeutics stabilize the β-sheet/Ser-273 region and inhibit Cdk5-mediated phosphorylation while minimally invoking adipogenesis and classical agonism, is indeed a valid framework to develop improved PPARγ modulators that retain antidiabetic actions while minimizing untoward effects.

As the prevalence of obesity continues to rise, therapies to treat metabolic syndrome and its associated conditions are of increasing importance. Thiazolidinediones (TZDs),[8] such as pioglitazone and rosiglitazone, are synthetic insulin-sensitizing

⌘ *Author's Choice*—Final version full access.
[S] This article contains supplemental Tables 1 and 2 and Figs. S1–S7.
The atomic coordinates and structure factors (code 3T03) have been deposited in the Protein Data Bank, Research Collaboratory for Structural Bioinformatics, Rutgers University, New Brunswick, NJ (http://www.rcsb.org/).
[1] These authors contributed equally to this work.
[2] The Molecular Pharmacology Laboratory Group was supported by MCT/CNPq/CT-Infra/CT-Grant 620195/2008-8 and 485811/2011-1.
[3] Supported by Fundação de Amparo a Pesquisa do Estado de São 598 Paulo (FAPESP) Grant 2010/17048-8.
[4] Supported by FAPESP Grant 2010/08680-2.
[5] Supported by FAPESP Grant 2009/14108-2.
[6] To whom correspondence may be addressed. Tel.: 713-441-2553; E-mail: kphillips@tmhs.org.
[7] To whom correspondence may be addressed. Tel.: 55-61-3072098; E-mail: nevesfar@gmail.com.

[8] The abbreviations and trivial name used are: TZD, thiazolidinedione; LBD, ligand-binding domain; PPAR, peroxisome proliferator-activated receptor; hPPAR, human PPAR; ITT, insulin tolerance test; HFD, high fat diet; WAT, white adipose tissue; HDX, hydrogen/deuterium exchange; MD, molecular dynamics; GQ-16, 5-(5-bromo-2-methoxy-benzylidene)-3-(4-methyl-benzyl)-thiazolidine-2,4-dione.

drugs that are highly effective in treating insulin resistance and type 2 diabetes (1). Unfortunately, the use of TZDs has been beset by insidious side effects, including weight gain, edema, cardiovascular toxicity (2), and bone loss (3). The Food and Drug Administration recently restricted the use of rosiglitazone due to an increased risk of cardiovascular events, underscoring a need for new medications that achieve insulin sensitization without adverse cardiovascular effects.

TZDs are potent agonists of PPARγ, a transcription factor and nuclear hormone receptor that is often referred to as the master regulator of adipogenesis (4–6). The classical mechanism by which TZDs activate PPARγ is well established (7). Ligand binding induces a large conformational change in helix 12 of the ligand-binding domain (LBD) of the receptor (8). This remodeling of the LBD creates a hydrophobic cleft on the surface of the receptor that serves as a high affinity docking site for the recruitment of transcriptional coactivators. Although the mechanism of transcriptional activation may be well appreciated, the rationale for insulin sensitization has not been. First, why is the activation of a pro-obesogenic receptor beneficial in treating insulin resistance, a phenomenon closely linked to obesity? Further, significant efforts toward the development of PPARγ ligands have failed to demonstrate a clear correlation between receptor transcriptional activation and *in vivo* efficacy. In fact, one of the most tantalizing results of these efforts may have been the discovery of "partial agonists," ligands with only partial efficacy in activating PPARγ that maintain insulin-sensitizing actions. That many partial agonists were reported to have lesser side effects than the full agonist TZDs suggested that ligands could be developed that maintain the insulin sensitization of TZDs without the undesirable side effects; however, the rationale for doing so was unclear.

Recently, however, studies from Choi *et al.* (9) have shown that PPARγ phosphorylation at Ser-273 is linked to obesity and insulin resistance. Ser-273 phosphorylation results in the dysregulation of a subset of PPARγ target genes, such as adiponectin, that are known to be associated with insulin sensitization. Moreover, this study also suggested that both TZDs and partial agonists with anti-diabetic effects improve insulin sensitivity primarily by inhibiting Cdk5-mediated phosphorylation of PPARγ at Ser-273. Ser-273 phosphorylation seems to be distinct from classical transcriptional activation, which appears to mediate at least some of the undesirable side effects of chronic PPARγ activation.

Herein we report the development of a novel PPARγ-targeted ligand that displays robust anti-diabetic activity in mice yet is dissociated from the TZD-related side effects of weight gain and edema. Structural and biochemical analyses allowed us to relate ligand binding mode to the desirable pharmacology and suggest that the *in vivo* efficacy of this compound arises from its ability to selectively and strongly stabilize the β-sheet region of the receptor, thus inhibiting Ser-273 phosphorylation by the Cdk5 kinase, as originally proposed by Choi *et al.* (9). These results may assist in the development of novel PPARγ modulators with decreased side effects.

EXPERIMENTAL PROCEDURES

Materials—GQ-16 (5-(5-bromo-2-methoxy-benzylidene)-3-(4-methyl-benzyl)-thiazolidine-2,4-dione) was synthesized in a manner similar to that previously described (10). Pioglitazone, troglitazone, bezafibrate, and 9-*cis*-retinoic acid were from Sigma, and rosiglitazone was from Cayman Chemical (Ann Arbor, MI). Pioglitazone, troglitazone, and rosiglitazone were sequentially used as positive controls for PPAR activation due to availability issues. Anti-aP2, anti-GAPDH, HRP-conjugated anti-mouse, and anti-goat IgGs were purchased from Santa Cruz Biotechnology, Inc. (Santa Cruz, CA). [^{3}H]rosiglitazone was from American Radiolabeled Chemicals (St. Louis, MO).

Transactivation Assays—Human promonocyte U-937 cells were transiently cotransfected with a plasmid containing the PPARγ LBD fused to the Gal4 DNA-binding domain and a plasmid containing the luciferase reporter gene under regulation by five Gal4 DNA-binding elements (UASG × 5 TK-luciferase). Transfections were performed by electroporation, and cells were treated with vehicle (DMSO) or compounds for 24 h at 37 °C. A reporter luciferase assay kit (Promega) was used to measure luciferase activity according to the manufacturer's instructions, with a luminometer (Turner). Each experiment was performed in triplicate and repeated at least three times. Results were reported as -fold induction of normalized luciferase activity ± S.E.

PPARγ Competition Binding Assay—His-LBD-hPPARγ was incubated for 12 h at 4 °C with 40 nM [^{3}H]rosiglitazone (specific activity 50 Ci/mmol) in buffer containing 10 mM Tris, pH 8.0, 50 mM KCl, and 10 mM dithiothreitol, in a final volume of 100 μl. Vehicle or unlabeled ligands were then added and allowed to incubate for an additional 12 h at 4 °C. Bound radioactive ligand was separated from free radioactivity by gravity flow-through 1-ml Sephadex G-25 desalting columns and quantitated using a liquid scintillation counter. K_i values were calculated using the one-site competition model in GraphPad 4.0 software (GraphPad, San Diego, CA). Similar methods were used initially to determine the K_d value of [^{3}H]rosiglitazone to be 33 nM.

Coactivator Interaction Assay—Full-length PPARγ was labeled with [^{35}S]methionine using a coupled *in vitro* transcription/translation system (Promega). GST and GST-SRC1(381–882) were expressed in *Escherichia coli* BL21 cells and purified using glutathione-Sepharose 4B beads. The interaction reaction was carried out as follows. Three ml of [^{35}S]methionine-labeled PPARγ were incubated with the glutathione bead suspension containing 4 mg of GST or GST-SRC1 fusion protein in GST-binding buffer (1× TST buffer with 0.1% Nonidet P-40, 0.1% Triton X-100, 1 mM DTT, and 2 g/ml bovine serum albumin) in the presence of vehicle or the indicated ligands in a final volume of 150 ml. After 2 h on a nutator at 4 °C, the beads were washed three times with 1 ml of GST-binding buffer. Bound proteins were eluted in 2× SDS loading buffer and resolved in 10% SDS-PAGE. After electrophoresis, the gels were fixed in 10% acetic acid (v/v), 40% methanol (v/v) for 30 min; treated in Amplify (Amersham Biosciences) for 30 min; and dried under vacuum for 2 h at 80 °C. Labeled PPARγ was then visualized by autoradiography.

Adipocyte Differentiation Assay, Oil Red O Staining, and Immunoblotting—Murine mesenchymal C3H10T1/2 cells or mouse embryonic fibroblast NIH-3T3L1 cells were cultured in DMEM supplemented with 10% fetal bovine serum, 2 mM glutamine, 50 units/ml penicillin, and 50 g/ml streptomycin and maintained at 37 °C and 5% CO_2. Two-day postconfluent cells (day 0) were induced to differentiate by incubation with DMEM supplemented with 1 μg/ml insulin (Sigma), 0.5 mM 3-isobutyl-1-methylxanthine (Sigma), and 1 μM dexamethasone (Sigma) for 2 days, followed by incubation with medium supplemented with 1 μg/ml insulin for 2 days. After this, cells were maintained in cell culture medium, changed every second day, until processing for analysis. Vehicle, 10 mM rosiglitazone, or 10 mM GQ-16 was added to the medium throughout the differentiation period (from day 0 to 2). Adipogenesis was assessed by staining intracellular lipids with Oil Red O, as described (11), and by immunoblotting for the adipocyte-specific marker aP2.

Mouse Protocols and Western Blots of Insulin Signaling Pathways—The ethics committee of the University of Campinas approved all animal protocols. Male Swiss mice were obtained from the University of Campinas Central Animal Breeding Center. Twelve-week-old mice that had been fed a high fat diet consisting of 55% calories from fat, 29% from carbohydrate, and 16% from protein (produced by the University of Campinas Central Animal Breeding Center; supplemental Table 1) since the age of 4 weeks were randomly assigned to receive vehicle, rosiglitazone (4 mg/kg/day), or GQ-16 (20 mg/kg/day) by oral gavage daily (n = 6/group). After 10 or 12 days of treatment, mice were submitted to either an insulin tolerance test (ITT) or intraperitoneal glucose tolerance test, respectively. All mice were weighed at 12 days. For the ITT, 1.5 IU/kg of human recombinant insulin (Humulin R) from Lilly was injected intraperitoneally, and serum glucose was measured at 0, 5, 10, 15, 20, 25, and 30 min thereafter. Glucose disappearance rate (K_{itt}) was calculated as described previously (12). For the intraperitoneal glucose tolerance test, glucose was administered intraperitoneally at a dose of 1 g/kg body weight, and serum glucose was measured at 0, 15, 30, 60, 90, and 120 min. After 15 days, mice were anesthetized by intraperitoneal injection of sodium thiopental, and anesthesia was confirmed by the loss of pedal and corneal reflexes. Insulin was then injected (3.8 IU/kg intravenously), and 5 min later, muscle, adipose tissue, and liver extracts were used for immunoblotting with the following antibodies: anti-insulin receptor, anti-phosphorylated insulin receptor, anti-insulin receptor substrate 1, anti-phosphorylated insulin receptor substrate 1, anti-JNK (Santa Cruz), anti-protein kinase B, anti-phosphorylated protein kinase B, and anti-IκBα (Cell Signaling).

Energy Balance Studies—Male C57Bl/6J mice at 6 weeks of age were fed a Western diet (45% kcal fat, D12079, Research Diets) for 10 weeks. Metabolic rate, food intake, and ambulatory activity were measured using the comprehensive laboratory animal monitoring system from Columbus Instruments (Columbus, OH). Mice were housed in individual metabolic cages with food and water *ad libitum* and allowed to acclimate for 48 h prior to the start of data collection. Mice were administered vehicle, rosiglitazone (4 mg/kg/day), or GQ-16 (20 mg/kg/day) via intraperitoneal injection. Energy expenditure, food intake and ambulatory activity were examined and reported as an average over 3 days. After 7 days, fat and lean body mass were measured by quantitative NMR, and hematocrit levels were measured following capillary centrifugation.

Cdk5 Phosphorylation of PPARγ LBD—Purified PPARγ LBD was bound to HisTrap magnetic beads (Invitrogen) and incubated with active Cdk5 p35 (Sigma) in 70 mM Tris, pH 7.6, 10 mM $MgCl_2$, 5 mM DTT, and 1 μM ATP for 1 h, after which the beads were washed three times with wash buffer, containing 20 mM Tris, pH 8, 150 mM NaCl, and 0.1% Triton X-100. Proteins were resolved by SDS-PAGE, and PPARγ phosphorylation was assessed by autoradiography.

Protein Preparation and Crystallization—The N-terminal His_6-tagged PPARγ LBD construct was transformed into BL21 cells grown in LB at 37 °C to an OD of 0.6. Expression was induced with 0.5 mM isopropyl 1-thio-β-D-galactopyranoside, and cells were grown at 18 °C overnight. Cells were harvested by centrifugation, lysed via sonication, and purified using a GE Hiprep Ni^{2+}-NTA affinity column via the manufacturer's standard protocol and eluted with 500 mM imidazole. The fraction containing pure PPARγ LBD was buffer-exchanged into 25 mM Tris buffer at pH 7.5 containing 150 mM NaCl using a desalting column. The protein·drug complex was prepared by adding a saturated solution of GQ-16 in DMSO to a 1:2 PPARγ-LBD/SRC1-peptide (LTERHKIL-HRLLQEGSPS) solution. After mixing, the final concentration of GQ-16 was ~600 mM. The complex was incubated at room temperature overnight and then concentrated to a final protein concentration of 10 mg/ml. The protein·ligand complex was crystallized at room temperature using the hanging drop vapor diffusion method by mixing equal volumes of the above complex and the reservoir solution containing 0.2 M ammonium acetate, 0.1 M sodium citrate at pH 5.6, and 30% PEG 4000. X-ray data were collected at the Advanced Light Source (ALS) Beamline 5.0.1. Data processing and scaling was done using IMOSFLM and SCALA module in CCP4 (13), and the structure was refined via the PHASER molecular replacement (14) module in PHENIX (15) to 2.1 Å. Coot (16) was used to visualize experimental electron density maps and for model building. Selected intensity data and refinement statistics are given in supplemental Table 2. All figures were prepared using PyMOL software (Schrödinger LLC, New York).

Hydrogen/Deuterium Exchange Mass Spectrometry of PPARγ LBD—Mass spectroscopy experiments were conducted using apo-hPPARγ LBD and hPPARγ LBD in the presence of rosiglitazone and GQ-16 (1.5-fold molar excess of ligand). Hydrogen/deuterium exchange mass spectrometry experiments were initiated by 20-fold dilution of hPPARγ in D_2O buffer (final buffer: 1 mM Hepes, 7.5 mM NaCl, 0.2% glycerol, 0.1 mM DTT, and 60% (v/v) D_2O) at 25 °C. These mixtures were incubated for 0, 1, 5, 30, and 90 min. Hydrogen/deuterium exchange was halted at each time point by placing samples on ice and adding 10 mM phosphate buffer (pH 2.5). The protein was immediately submitted to cleavage with pepsin (10 μg) for 7 min at 4 °C to decrease the rate of solvent back-exchange. After the addition of 30% acetonitrile, the samples were immediately applied onto

a Synapt G2 HDMS (Waters) by direct infusion. The software MS-Digest (17) was used to identify the sequence of the peptic peptide ions, generated by pepsin cleavage. Deuterium level for each peptide was determined from the differences in centroid masses between the deuterated and non-deuterated fragments (18). The non-digested protein, after deuteration, was used as a control to estimate deuterium loss during protein digestion. This procedure was applied to both liganded and unliganded protein.

Molecular Dynamics Simulations—The simulations started from the crystallographic structure presented in this work (chain B of the GQ-16 complex) and from the structure 1FM6 (19) (chain D of the rosiglitazone complex) from the PDB. Missing residues in the GQ-16 complex structure (206–209 and 258–276) were taken from the structure of the rosiglitazone complex, which fit well after structural alignment with LovoAlign (20). Hydrogen atoms were added, and the protonation states of the histidine residues were estimated with H++ (21) at pH 7. For all of the neutral histidines, the position of the hydrogen atoms was defined in such a way as to favor hydrogen bonds. The systems were then fully solvated with a water shell of at least 15 Å and neutralized with sodium and chloride ions to a total concentration of 0.15 mol/liter using the vmd (22) plugins solvate and autoionize, respectively. The final systems contained around 58,000 atoms.

The CHARMM force field (23) was used for the protein, and the TIP3P (24) model was used for water molecules. Force field parameters for rosiglitazone were obtained as described previously (25), and GQ-16 was parameterized consistent with this protocol. The simulations were performed using periodic boundary conditions in the NpT ensemble 300 K and 1 atm using the Langevin thermostat and the Langevin/Nosé-Hoover piston for the temperature and pressure control, respectively. Electrostatics was evaluated using the particle mesh Ewald (26) algorithm, and short range interactions were truncated at a cutoff radius of 12 Å. All of the bonds involving apolar hydrogens were constrained at their equilibrium values using SHAKE (27), and a time step of 2.0 fs was used for the integration of the equations of motion.

The following treatment was used to prepare the systems for the production runs: (*a*) 2000 energy minimization steps using the conjugate gradients algorithm (CG) followed by 200 ps of MD keeping the ligand and protein residues fixed, except modeled residues; (*b*) 1000 energy minimization steps using CG followed by 200 ps of MD keeping only α carbons fixed (except those modeled); (*c*) 600 ps of MD without any constraints. After these preparative steps, MD trajectories of 5.0 ns were generated for analysis. This protocol was repeated five times for each system using the program NAMD (28).

Statistical Analysis—Data handling, analysis, and graphical representations were performed using GraphPad 4.0 software (GraphPad, San Diego, CA). Statistical differences were determined by one-way analysis of variance followed by Student-Newman-Keuls multiple comparison or by Student's *t* test; $p < 0.05$ was accepted as statistically significant.

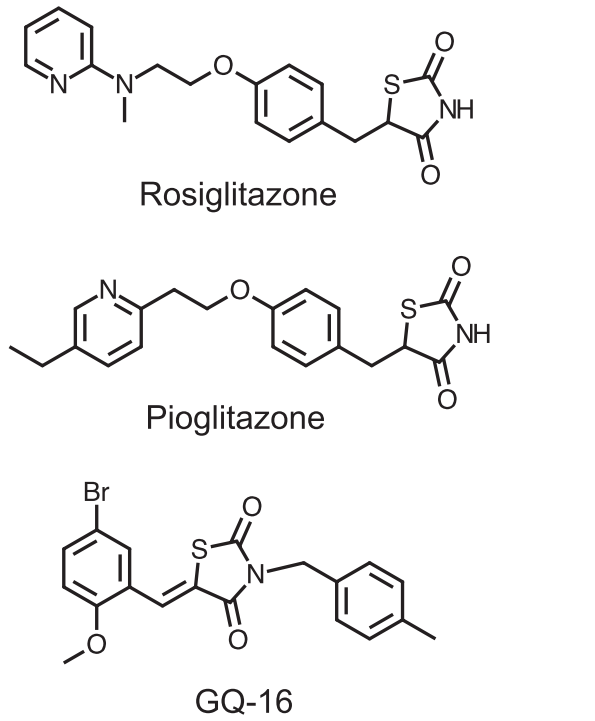

FIGURE 1. **Chemical structure of GQ-16 compared with TZDs rosiglitazone and pioglitazone.**

RESULTS

GQ-16 Is Partial Agonist of PPARγ with Reduced Adipogenic Actions—We previously described a series of 5-benzylidene-4-(4-methyl-benzyl)-thiazolidine-2,4-dione derivatives substituted on the benzylidene moiety (29) that included the ligand GQ-2. As an extension of this effort we synthesized the related compound GQ-16 (Fig. 1). GQ-16 was found to be a moderate affinity ligand for the LBD of PPARγ, exhibiting a K_i of 160 nM (supplemental Fig. S1*A*). GQ-16 was specific for PPARγ and possessed no detectable activity when tested for the ability to activate other PPAR subtypes (PPARα or PPARβ/δ) or RXRα (supplemental Fig. S1*B*). In transactivation assays, GQ-16 acted as a weak partial agonist. Even high concentrations of GQ-16 elicited only approximately one-third of the maximal activation stimulated by rosiglitazone (Fig. 2*A*). *In vitro* binding studies performed in the presence of saturating concentrations of ligand demonstrated that GQ-16 is significantly less effective in promoting the interaction between PPARγ and SRC-1 than the TZD troglitazone (supplemental Fig. S2). Finally, GQ-16 displayed reduced adipogenic potential in both NIH-3T3 and C3H10T1/2 cells, established models of PPARγ-dependent adipogenesis. Intracellular lipid accumulation afforded by GQ-16 and induction of the adipocyte-specific marker aP2 was less than that obtained with rosiglitazone (Fig. 2, *B* and *C*). Collectively, these results suggest that the binding of GQ-16 to PPARγ induces a receptor conformation that is suboptimal for the recruitment of coactivators to the AF-2 surface of the receptor.

GQ-16 Improves Insulin Sensitivity without Promoting Weight Gain—We next tested the anti-diabetic properties of GQ-16 in a mouse model of diet-induced obesity and insulin resistance and compared its effects to rosiglitazone. Both

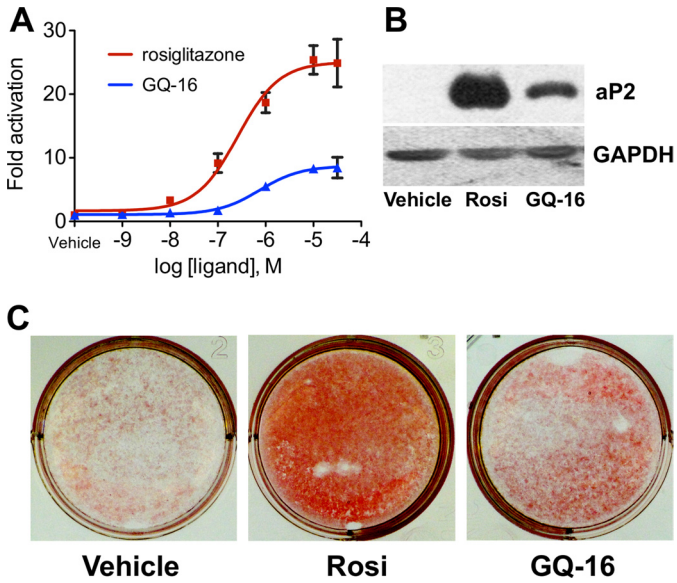

FIGURE 2. **GQ-16 is a partial agonist of PPARγ with modest adipogenic activity.** *A, in vitro* transactivation of a PPARγ-based reporter with either rosiglitazone (*squares*) or GQ-16 (*triangles*). *B* and *C*, GQ-16 (10 μM) induces adipogenesis to a lesser extent than rosiglitazone (*Rosi*; 10 μM) in both C3H10T1/2 (*B*) and NIH-3T3-L1 cells (*C*), as indicated by Western blot of the adipogenic marker protein aP2 (*B*) and Oil Red staining (*C*). *Error bars*, S.E.

GQ-16 and rosiglitazone reversed high fat diet (HFD)-mediated impairments in insulin signaling as indicated by an increase in phosphorylation of the insulin receptor (*IR*; Fig. 3, *A–C*), insulin receptor substrate 1 (*IRS-1*; Fig. 3, *D–F*), and protein kinase B (*Akt*; Fig. 3, *G–I*) in adipose tissue, liver, and muscle. GQ-16 and rosiglitazone also exhibited equivalent capacity to block HFD-dependent effects on intracellular inflammatory pathways related to insulin resistance. Both ligands reversed HFD-dependent suppression of inhibitor of nuclear factor κB (IκBα) protein in the adipose tissue, liver, and muscle of HFD-fed mice when compared with chow-fed controls (Fig. 3, *J–L*). Further, GQ-16 and rosiglitazone reduced HFD-dependent phosphorylation of JNK, a marker of inflammatory signaling in adipose tissue, liver, and muscle (Fig. 3, *M–O*). Remarkably, although GQ-16 treatment resulted in improved insulin sensitivity, as indicated by a greater plasma glucose disappearance rate (K_{itt}) (Fig. 4*A*), and glucose tolerance (Fig. 4*B*), GQ-16 did not elicit increased weight gain (Fig. 4*C*), a common side effect of TZD treatment.

Unlike Rosiglitazone, GQ-16 Does Not Induce Edema—In order to establish how GQ-16 acts as a PPARγ agonist without evoking the associated side effect of weight gain, we sought to determine which aspects of energy balance and contributing factors to weight gain might be differentially regulated by GQ-16 and rosiglitazone. Because rosiglitazone is known to stimulate weight gain via two primary mechanisms (hyperphagia, which has recently been shown to have a neurological basis (30, 31), and edema, which is mediated by a PPARγ-driven increase in water retention by the kidneys (32)), we examined the effects of rosiglitazone and GQ-16 on food intake and hemodilution. Treatment with either rosiglitazone or GQ-16 for 7 days did not alter food intake (Fig. 4*D*) or activity and did not result in a detectable change in body composition (supplemental Fig. S3), although there was a statistically significant difference representing decreased fat mass in GQ-16-treated mice relative those treated with rosiglitazone. Conversely, treatment with rosiglitazone brought about a significant level of hemodilution, whereas hematocrit was unchanged following GQ-16 treatment (Fig. 4*E*). In addition to hyperphagia, recent studies have shown that PPARγ agonists can also affect energy balance in a positive fashion by increasing the oxidative metabolism, or inducing a "beiging," of white adipose tissue (WAT) (33). To examine whether GQ-16 brought about a beiging of WAT or increased energy expenditure by other means, indirect calorimetry was used to measure metabolic rate, and the expression of oxidative metabolic genes was measured in visceral and subcutaneous WAT as well as brown adipose tissue. Neither rosiglitazone nor GQ-16 afforded a detectable increase in energy expenditure (Fig. 4, *F* and *G*), and genes involved in the oxidative metabolism of adipose tissue were not significantly changed in either epididymal or inguinal WAT or brown adipose tissue (supplemental Fig. S4). However, several markers of oxidative metabolism in subcutaneous inguinal fat, such as Ucp1, Elovl3, and Pgc-1a, did tend to increase following treatment with either rosiglitazone or GQ-16, although high variability of the expression data precludes detailed analysis. Consequently, we cannot rule out the possibility that GQ-16 may exert its effects in part by increasing the oxidative metabolism of subcutaneous WAT. Thus, although GQ-16 appears to be a weak PPARγ agonist relative to rosiglitazone, it possesses efficient insulin-sensitizing actions *in vivo* that are separable from at least one of the deleterious effects of the TZDs, edema, and it may have additional beneficial effects on WAT metabolism.

GQ-16 Inhibits Cdk5 Phosphorylation of PPARγ Ser-273—Because the insulin-sensitizing effects of PPARγ ligands, such as rosiglitazone, appear to be more closely correlated with their ability to inhibit phosphorylation of Ser-273 than with classical receptor activation, we assessed the ability of GQ-16 to inhibit Cdk5 phosphorylation of PPARγ *in vitro*. GQ-16 blocked Ser-273 phosphorylation in a concentration-dependent fashion, with higher concentrations being as efficacious as rosiglitazone, affecting a complete inhibition of PPARγ phosphorylation (Fig. 4*H*).

X-ray Structural Analysis Reveals Unique GQ-16 Binding Mode Relative to TZDs and Other PPARγ Ligands—To better understand the structural basis for the unique pharmacologic profile of GQ-16, we determined the x-ray crystal structure of the GQ-16·PPARγ complex. In general, the complex appeared similar to previously reported structures of liganded PPARγ structures, with helix 12 in an active position and no noteworthy differences in overall LBD fold (Fig. 5, *A* and *B*). There were, however, significant differences in ligand binding mode. GQ-16 was found to bind to PPARγ in a fashion that is not only distinct from the binding mode of TZDs, such as rosiglitazone, but appears to be unique relative to nearly all other previously reported PPARγ structures (Fig. 5*C*). Although TZDs, such as rosiglitazone and pioglitazone, bind in a perpendicular fashion to helix 3, partially wrapping around the helix, GQ-16 binds in a north-south orientation, parallel to helix 3. Given this binding modality, GQ-16 does not make direct contact with any residues of helix 12 (Fig. 5*D*), a suggested hallmark of full agonists,

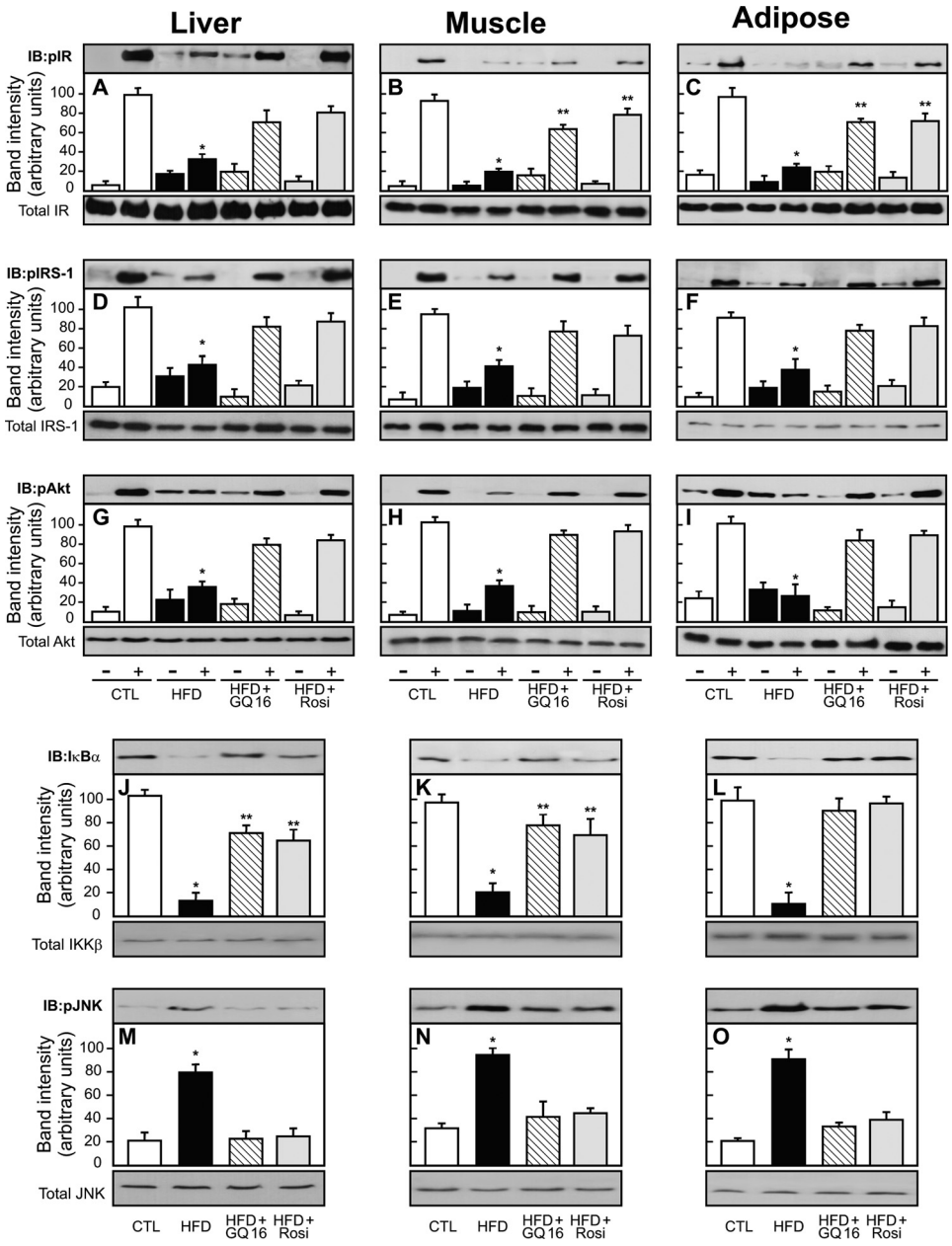

FIGURE 3. **GQ-16 improves insulin-signaling components in liver, muscle, and adipose tissue of obese Swiss mice.** *A–C*, insulin-induced tyrosine phosphorylation of the insulin receptor (*IR*); *D–F*, insulin-induced tyrosine phosphorylation of insulin receptor substrate 1 (*IRS-1*); *G–I*, insulin-induced serine phosphorylation of protein kinase B (*Akt*); *J–L*, IκBα protein levels; *M–O*, phosphorylation of JNK. The results of densitometry were expressed as arbitrary units. *IB*, immunoblot; *CTL*, control. *Bars*, mean ± S.E. (*error bars*).

such as the TZDs, which interact with the side chain of Tyr-501 on the inner surface of helix 12 via their TZD core (Fig. 5*E*). GQ-16 makes no polar contacts with PPARγ; instead, ligand positioning appears to be mediated by van der Waals interactions, water-mediated contacts, and π-stacking between the guanidinium side chain of Arg-316 and the tolyl group of GQ-16.

GQ-16 Strongly Stabilizes the β-Sheet/Ser-273 and Helix 3 Regions of PPARγ—In order to examine whether GQ-16 may block Cdk5-mediated phosphorylation of Ser-273 by stabilizing the β-sheet region of PPARγ, we carried out hydrogen/deuterium exchange (HDX) (34) experiments to explore structural dynamics of the receptor in solution. In the absence of ligand, helix 12 of the aporeceptor appears to be highly dynamic (Fig. 6 and supplemental Fig. S5), a fact that is well appreciated for nearly all nuclear receptors. However, high levels of exchange were not limited to helix 12 but were instead observed throughout the LBD of the aporeceptor. The lability of this state suggests that the unliganded receptor does not assume a single well ordered state but is instead "molten" prior to ligand-induced stabilization. The binding of either rosiglitazone or GQ-16 to PPARγ resulted in significant stabilization throughout the entire receptor, as indicated by a large decrease in the overall hydrogen/deuterium exchange (Fig. 6, *A* and *B*).

In particular, the helix 3, helix 12, and β-sheet regions of PPARγ were most highly affected by ligand binding. Although

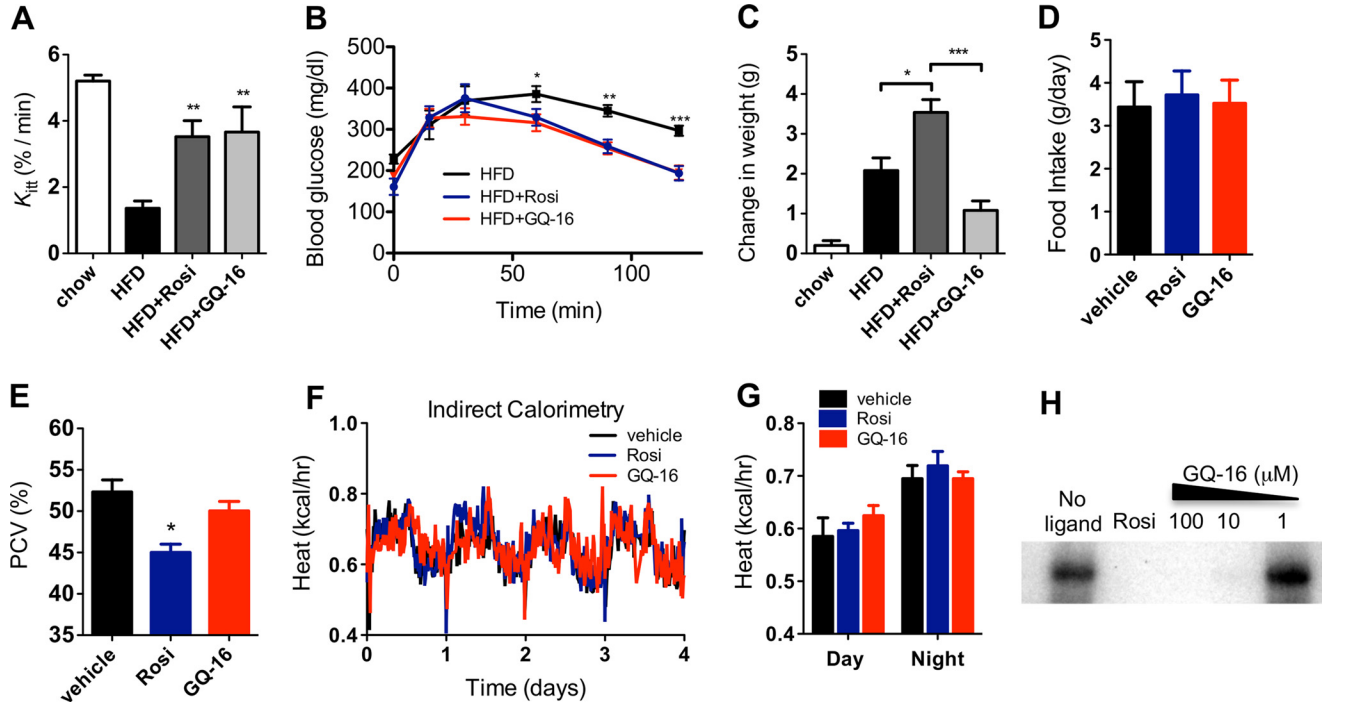

FIGURE 4. **GQ-16 improves insulin sensitivity without evoking weight gain and inhibits Cdk5 phosphorylation of PPARγ *in vitro*.** Shown are the short insulin tolerance test (*A*), intraperitoneal glucose tolerance test (*B*), and change in body weight (*C*) of mice treated with either DMSO, rosiglitazone (*Rosi*) (4 mg/kg/day), or GQ-16 (20 mg/kg/day) for 10 (*A*) or 12 days (*B* and *C*) ($n = 6$). The effect of rosiglitazone and GQ-16 on food intake (*D*) and hematocrit (*E*) is shown. *F* and *G*, indirect calorimetry of mice treated with either DMSO, rosiglitazone, or GQ-16 for 7 days. *G*, average heat over a 4-day period ($n = 4$). *H*, GQ-16 completely blocks phosphorylation of PPARγ by Cdk5 *in vitro*. *PCV*, packed cell volume. Shown is mean ± S.E. (*error bars*). Analysis was by one-way analysis of variance. *, $p < 0.05$; **, $p < 0.01$; ***, $p < 0.001$.

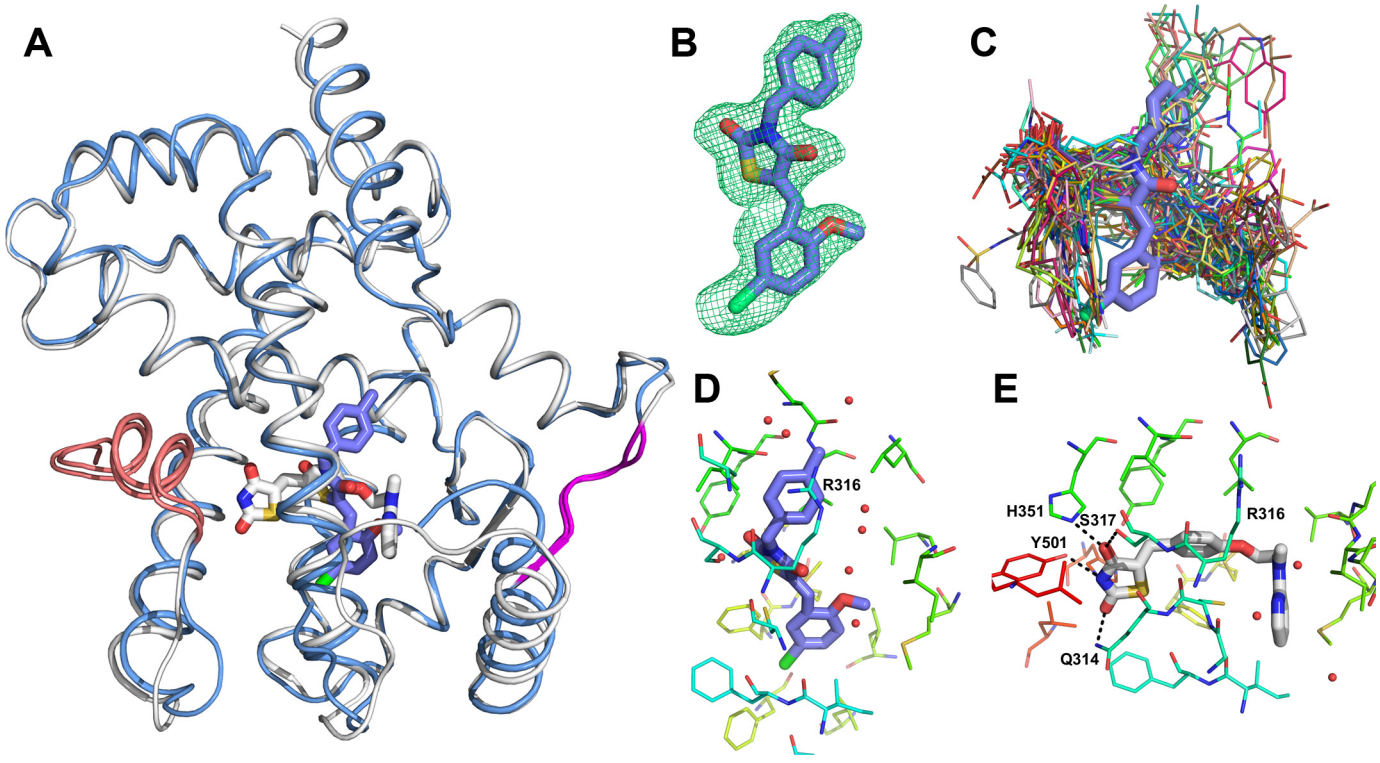

FIGURE 5. **GQ-16 interacts with PPARγ via a distinctive binding mode.** *A*, although GQ-16 (*purple*) induces an overall structure similar to that of rosiglitazone (*blue*, GQ-16·PPARγ; *white*, rosiglitazone·PPARγ) (Protein Data Bank entry 2PRG), GQ-16 binds to PPARγ in a different orientation than traditional TZDs, such as rosiglitazone. GQ-16 makes no direct contacts with residues of helix 12 (shown in *red*), a hallmark of traditional TZDs. The Cdk5 recognition site, which includes Ser-273, is shown in *magenta*. *B*, electron density of GQ-16 (SA-Composite Omit map; $F_o - F_c$) contoured at 2 s. *C*, superposition of GQ-16 and other reported PPARγ-ligand complex structures showing that GQ-16 uses a unique binding mode relative to other ligands. *D* and *E*, comparison of ligand-protein contacts between PPARγ and GQ-16 (*D*) or rosiglitazone (*E*) (polar contacts are shown as *dotted lines*).

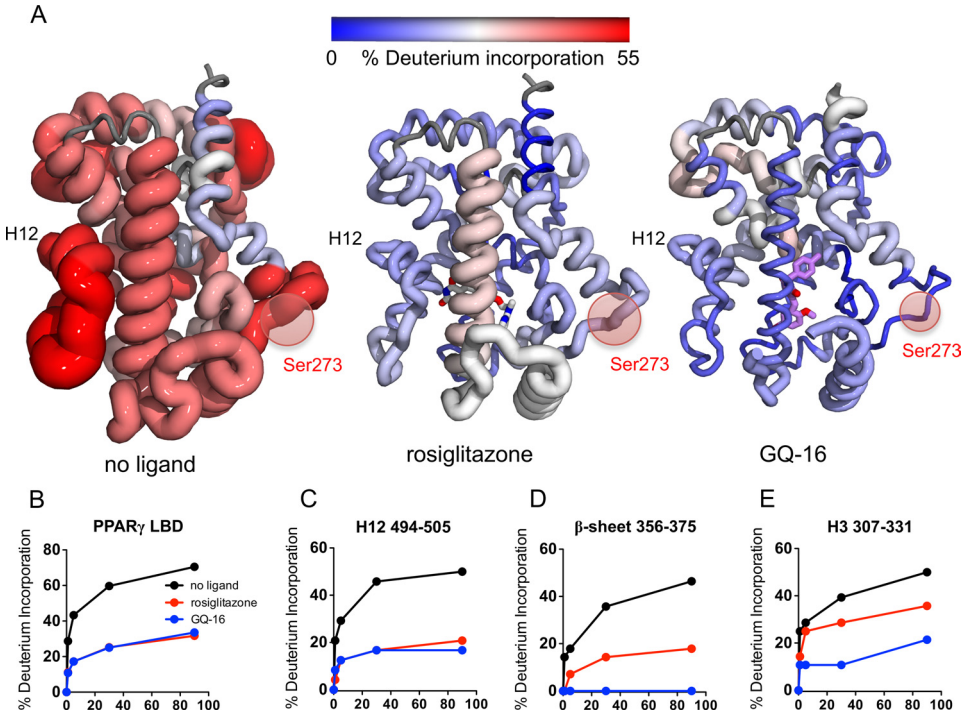

FIGURE 6. **GQ-16 strongly protects the helix 3 and β-sheet regions from hydrogen/deuterium exchange.** *A*, comparison of hydrogen/deuterium exchange levels after 30 min. In the absence of ligand, high levels of exchange are observed throughout the LBD. *B*, both rosiglitazone and GQ-16 strongly protect the overall LBD from exchange, although the pattern produced by each is distinct (*A*). *C–E*, although both ligands protect helix 12 similarly (*C*), GQ-16 more strongly protects the β-sheet (*D*) and helix 3 (*E*) regions from hydrogen/deuterium exchange.

both ligands stabilized the overall receptor and helix 12 to a similar extent, GQ-16 was more effective at protecting the lower half of the LBD, stabilizing the helix 11–12 loop, helix 3, and β-sheet/Ser-273 regions of PPARγ more strongly than rosiglitazone (Fig. 6, *C–E*). At most time points, GQ-16 protected the peptide representing the first β-strand/Ser-273 region more strongly than any other region of the LBD, revealing the potential of the Ser-273 region to act as a regulatory site and implying that the *in vivo* efficacy of GQ-16 stems from its ability to strongly stabilize this region, protecting it not only from solvent-mediated hydrogen/deuterium exchange but also from kinase accessibility to Ser-273.

Molecular Dynamics Simulations of Helix 12 Stabilization by GQ-16 and Rosiglitazone—To better understand differential effects of rosiglitazone and GQ-16 on PPARγ activity and stability, we performed molecular dynamics (MD) simulations with the structures of rosiglitazone and GQ-16 bound to PPARγ (Fig. 7). The simulations predicted that rosliglitazone binds to helix 12 through a direct hydrogen bond with the residue Tyr-501, in accordance with the crystal structure, and the occurrence of this bond was nearly 100% (Fig. 7, *A* and *C*). In contrast, GQ-16 attempted to recapitulate this interaction via the introduction of a loose, water-mediated contact with Tyr-501, which had an occurrence of about 60% during the simulations (Fig. 7, *B* and *C*). Correspondingly, there were somewhat larger fluctuations in the average position of helix 12 when PPARγ was occupied by GQ-16 than with rosiglitazone, indicated by broader and leftward shifted root mean square deviation values (Fig. 7*D*). However, these differences in root mean square deviation do not necessarily imply greater solvent accessibility of helix 12 because analysis of helix 12 hydration indicated that an average of 15 water molecules were involved in the solvation of both systems (supplemental Fig. S6).

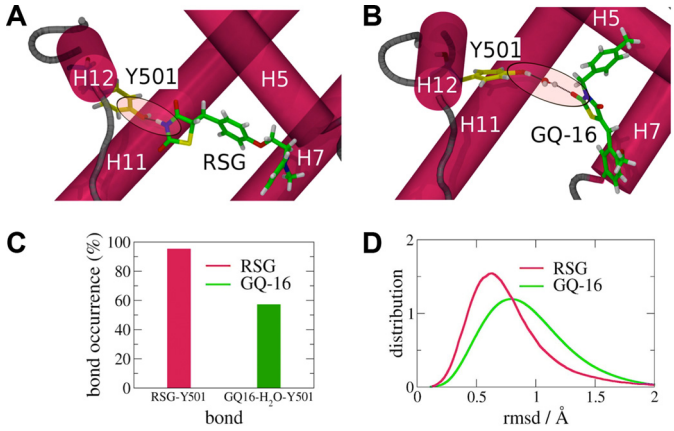

FIGURE 7. **Molecular dynamics simulations predict that GQ-16 stabilizes the active conformation of helix 12 less than rosiglitazone.** *A* and *B*, unlike rosiglitazone (*A*), GQ-16 (*B*) does not directly contact helix 12; instead a water molecule mediates an interaction between Tyr-501 of helix 12 and a carbonyl of GQ-16. *C*, this water-mediated interaction with helix 12 is weaker than the direct rosiglitazone-Tyr-501 interaction and exists less than 60% of the time during simulations. Rosiglitazone makes a direct contact with helix 12 via a hydrogen bond with the hydroxyl group of Tyr-501 (*B*) that is quite stable as the bond is maintained >90% of the time during simulations. *D*, helix 12 samples a broader ensemble of conformations when bound to GQ-16 relative to rosiglitazone (*RSG*).

DISCUSSION

PPARγ agonists, such as the TZDs pioglitazone and rosiglitazone, have proven efficacious as insulin-sensitizing agents in humans as well as in animal models of obesity and diabetes. Despite established therapeutic value, their clinical use is lim-

ited by adverse effects, such as weight gain, bone loss (3, 35–37), and increased cardiovascular risk (2). These limitations spurred a large effort to produce PPARγ targeted therapeutics that maintain insulin-sensitizing actions but are dissociated from the deleterious effects. Initially, side effects were thought to arise from off-target effects, leading to the subsequent development of numerous high affinity, high specificity PPARγ agonists. As a seeming paradox, increased potency appeared to maximize not only the insulin-sensitizing effects but also to amplify the untoward effects. It became evident that the connection between PPARγ activation and beneficial anti-diabetic actions was not straightforward, and efforts instead shifted toward the promise of partial agonists (38), PPARγ-directed agents that seemed to possess precisely the right magnitude of receptor agonism.

Under this paradigm of, "a little bit of activity, but not a lot," we developed a series of modified TZDs and then selected compounds with weak but definitive activity toward PPARγ for further study. GQ-2 proved to be effective as an orally available insulin-sensitizing agent (29) that did not induce weight gain. Although poor solubility of GQ-2 confounded cellular and biochemical studies, the closely related ligand GQ-16 was found to have similar efficacy *in vivo*, so further characterization efforts focused on GQ-16.

Although we initially assumed that GQ-16 simply possessed a better balance of agonism and antagonism than traditional TZDs, recent work by Choi *et al.* (9, 39) suggested a novel, mechanistic explanation for the insulin-sensitizing actions of PPARγ partial agonists, forcing us to reevaluate the rationale for our success. The authors provide evidence that the insulin-sensitizing effects of TZDs are not related to classical agonist activity but are consequences of a second effect, the ligand-dependent inhibition of Ser-273 phosphorylation by the Cdk5 kinase. This inhibition enhances insulin sensitivity by reversing Cdk5-mediated attenuation of a subset of beneficial PPARγ-regulated genes, including the adipokine adiponectin (40). Ser-273, which is located immediately adjacent to the first β-strand of PPARγ, is far removed from the AF-2 activation surface. Intriguingly, the β-sheet region has been shown to mediate interprotein contacts between PPARγ and its heterodimeric partner, RXR (41). Mutation to this region decreases the affinity of the PPARγ·RXR complex for its response element as well as reducing its transcriptional activity. Phosphorylation of Ser-273 may similarly disrupt contacts between PPARγ and RXR, potentially reducing the transcriptional response from promoters for which this interaction is constructive. From this new perspective, the convolution of "partial agonism" arises from PPARγ ligands that are differentially effective in inhibiting the phosphorylation of Ser-273 relative to their ability to elicit classical AF-2-mediated activation. Moreover, this model suggests that an "ideal" partial agonist would block Cdk5 phosphorylation of PPARγ while minimally invoking classical activation or adipogenesis.

Is the *in vivo* efficacy of GQ-16 due to this type of "idealized" selective PPARγ modulation? Although it is difficult to prove that the positive pharmacological profile of GQ-16 results solely from the selective inhibition of Cdk5-mediated phosphorylation of PPARγ, our results are largely consistent with this model. Even at saturating doses, GQ-16 is significantly less efficient than TZDs in activating PPARγ in transactivation assays, inducing association with coactivators *in vitro*, and driving adipogenesis and the expression of adipogenic markers, such as aP2. Nevertheless, GQ-16 appears to be even more highly effective than rosiglitazone at stabilizing the helix 3 and β-sheet regions of PPARγ and has similar efficacy in blocking phosphorylation by Cdk5 and improving insulin sensitivity *in vivo*, all without invoking attendant weight gain. Taken as a whole, it appears unlikely that the modest ability of GQ-16 to initiate transcription via "classical" means is the only factor responsible for its pharmacological efficacy, which more likely stems from both its weak classical agonist properties and its ability to strongly stabilize the β-sheet region of PPARγ and occlude Ser-273 from Cdk5 accessibility.

Structural studies indicated that GQ-16 interacts with PPARγ via a binding mode that is unique relative to other reported PPARγ-ligand structures. The positioning of GQ-16 deep in the binding pocket, out of contact with helix 12, utilizing a north-south binding orientation, bears no resemblance to the binding mode of TZDs and other full agonists but is most closely related to partial agonists, such as PA-082 (42), MRL-24, nTZDpa, and BVT.13 (43). Although the positioning of these ligands within the binding pocket differs to a certain extent, none of these ligands interact directly with helix 12. Instead, all of the compounds bind parallel to helix 3 (supplemental Fig. S7). Similar to our results with GQ-16, Bruning *et al.* (43) used HDX to show that MRL-24, nTZDpa, and BVT.13 all stabilize the helix 3 and β-sheet regions of PPARγ even more strongly than rosiglitazone. Presumably, the binding orientation of these compounds, which allows for extensive contact between ligand and helix 3, is responsible for the increased stabilization of this helix. Ligand binding to PPARγ seems to induce a cooperative folding transition between the helix 3 and β-sheet regions because the stability of these structural elements appears to be strongly correlated. Because the Cdk5 recognition site extends into the first β-strand of PPARγ, structural stabilization of the β-sheet region, elicited by GQ-16 and other ligands, presumably renders Ser-273 inaccessible to the kinase, protecting the receptor from phosphorylation.

HDX studies indicated that helix 12 exhibits similar solvent accessibility when the LBD is bound to either GQ-16 or rosiglitazone. This was unexpected in light of the weak agonist activity of GQ-16 and the lack of direct interactions between the ligand and Tyr-501. Although MD simulations should generally be treated as suggestive, these simulations can provide useful insights into conformational changes and other dynamical features of a biomolecular system when a good structural model is available. MD simulations of the GQ-16·PPARγ complex suggest that GQ-16 uses a bridging water molecule to interact with Tyr-501 and that this interaction stabilizes helix 12 sufficiently that it remains docked with the body of the receptor and is protected from solvent exposure. However, this water-mediated stabilization is not sufficient to fully secure the active conformation of the receptor, leading to suboptimal conformational restraint of the AF-2 activation surface. Thus, the MD simulations suggest a potential rationale for the discrepancy between the HDX results, where GQ-16 appears to stabilize helix 12 as effectively as rosiglitazone, and the functional stud-

ies, where GQ-16 is clearly not as efficacious as rosiglitazone at eliciting classical PPARγ activation. If this suggestion is correct, MD simulation studies may be able to assist in the design of GQ-16 derivatives that differ in their ability to stabilize helix 12 via this bridging interaction while maintaining their ability to stabilize the β-sheet/S273 region of the receptor.

Although PA-082 and MRL-24 were originally chosen for comparison with GQ-16 based solely on the similarities of their ligand binding orientations (supplemental Fig. S7), the pharmacological profiles reported for each are remarkably similar to that of GQ-16. Both are weak agonists of PPARγ that have been reported to act as insulin sensitizers without eliciting weight gain attendant to rosiglitazone or pioglitazone treatment (42, 44). These similarities suggest a strategy for drug design, and GQ-16 could represent an attractive lead compound for further development. Although GQ-16 has only modest affinity for PPARγ, the compound is orally active and displays excellent insulin-sensitizing actions. Further, the crystallographic structure of GQ-16·PPARγ suggests approaches by which to increase the compound's affinity and to potentially further separate ligand-dependent stabilization of the β-sheet/Ser-273 region from that of helix 12/AF-2. For example, functional groups that improve direct contacts between GQ-16 and the inner surface of the LBD at the helix 3/β-sheet region could enhance affinity while retaining stabilizing influence on the β-sheet region, and strategies to reduce water-mediated influences on helix 12 may further reduce classical partial agonist actions.

It will be important to determine the extent to which complete separation of these effects is possible and desirable. Although pure PPARγ classical agonism appears undesirable, the extent to which it is important to completely separate ligand effects on suppression of Cdk5-dependent phosphorylation at Ser-273 from helix 12 stabilization remains questionable. Some amount of adipogenesis may be advantageous; transgenic mice that overexpress the PPARγ target gene adiponectin experience an expansion of fat mass, which is tied to dramatic improvements in insulin sensitivity (45). Further studies of partial agonists like GQ-16 may help to address this question. Nevertheless, our analysis of the pharmacological profile of GQ-16 lends weight to the conceptual framework for selective PPARγ modulator development proposed by Choi *et al.* (9, 39). PPARγ ligands that selectively stabilize the β-sheet region, shielding Ser-273 from Cdk5-mediated phosphorylation while minimally invoking classical activation, appear to retain insulin-sensitizing actions yet display reduced harmful side effects. Continued efforts toward this end may lead to the development of effective insulin sensitizers with improved safety profiles.

Acknowledgments—We thank Dr. Carlos Pantoja for invaluable assistance with the adipogenesis studies, Rilva Soares Pinho Grigório for excellent technical assistance, and Eduardo J. Pilau and Fabio C. Gozzo of the Dalton Mass Spectrometry Group at UNICAMP for assistance with the HDX studies. The Berkeley Center for Structural Biology is supported in part by National Institutes of Health, NIGMS, and the Howard Hughes Medical Institute. The Advanced Light Source is supported by the Director, Office of Science, Office of Basic Energy Sciences, of the United States Department of Energy under Contract DE-AC02-05CH11231.

REFERENCES

1. Lehmann, J. M., Moore, L. B., Smith-Oliver, T. A., Wilkison, W. O., Willson, T. M., and Kliewer, S. A. (1995) An antidiabetic thiazolidinedione is a high affinity ligand for peroxisome proliferator-activated receptor γ (PPARγ). *J. Biol. Chem.* **270,** 12953–12956
2. Nissen, S. E., and Wolski, K. (2007) Effect of rosiglitazone on the risk of myocardial infarction and death from cardiovascular causes. *N. Engl. J. Med.* **356,** 2457–2471
3. Grey, A., Bolland, M., Gamble, G., Wattie, D., Horne, A., Davidson, J., and Reid, I. R. (2007) The peroxisome proliferator-activated receptor-γ agonist rosiglitazone decreases bone formation and bone mineral density in healthy postmenopausal women. A randomized, controlled trial. *J. Clin. Endocrinol. Metab.* **92,** 1305–1310
4. Morrison, R. F., and Farmer, S. R. (2000) Hormonal signaling and transcriptional control of adipocyte differentiation. *J. Nutr.* **130,** 3116S–3121S
5. Tontonoz, P., Hu, E., and Spiegelman, B. M. (1994) Stimulation of adipogenesis in fibroblasts by PPARγ2, a lipid-activated transcription factor. *Cell* **79,** 1147–1156
6. Willson, T. M., Lambert, M. H., and Kliewer, S. A. (2001) Peroxisome proliferator-activated receptor γ and metabolic disease. *Annu. Rev. Biochem.* **70,** 341–367
7. Nolte, R. T., Wisely, G. B., Westin, S., Cobb, J. E., Lambert, M. H., Kurokawa, R., Rosenfeld, M. G., Willson, T. M., Glass, C. K., and Milburn, M. V. (1998) Ligand binding and co-activator assembly of the peroxisome proliferator-activated receptor-γ. *Nature* **395,** 137–143
8. Nagy, L., and Schwabe, J. W. (2004) Mechanism of the nuclear receptor molecular switch. *Trends Biochem. Sci.* **29,** 317–324
9. Choi, J. H., Banks, A. S., Estall, J. L., Kajimura, S., Boström, P., Laznik, D., Ruas, J. L., Chalmers, M. J., Kamenecka, T. M., Blüher, M., Griffin, P. R., and Spiegelman, B. M. (2010) Anti-diabetic drugs inhibit obesity-linked phosphorylation of PPARγ by Cdk5. *Nature* **466,** 451–456
10. da Costa Leite, L. F., Veras Mourão, R. H., de Lima Mdo, C., Galdino, S. L., Hernandes, M. Z., de Assis Rocha Neves, F., Vidal, S., Barbe, J., and da Rocha Pitta, I. (2007) Synthesis, biological evaluation and molecular modeling studies of arylidene-thiazolidinediones with potential hypoglycemic and hypolipidemic activities. *Eur. J. Med. Chem.* **42,** 1263–1271
11. Janderová, L., McNeil, M., Murrell, A. N., Mynatt, R. L., and Smith, S. R. (2003) Human mesenchymal stem cells as an *in vitro* model for human adipogenesis. *Obes. Res.* **11,** 65–74
12. Bonora, E., Moghetti, P., Zancanaro, C., Cigolini, M., Querena, M., Cacciatori, V., Corgnati, A., and Muggeo, M. (1989) Estimates of *in vivo* insulin action in man. Comparison of insulin tolerance tests with euglycemic and hyperglycemic glucose clamp studies. *J. Clin. Endocrinol. Metab.* **68,** 374–378
13. Collaborative Computational Project, Number 4 (1994) The CCP4 suite. Programs for protein crystallography. *Acta Crystallogr. D Biol. Crystallogr.* **50,** 760–763
14. McCoy, A. J., Grosse-Kunstleve, R. W., Adams, P. D., Winn, M. D., Storoni, L. C., and Read, R. J. (2007) Phaser crystallographic software. *J. Appl. Crystallogr.* **40,** 658–674
15. Adams, P. D., Afonine, P. V., Bunkóczi, G., Chen, V. B., Davis, I. W., Echols, N., Headd, J. J., Hung, L. W., Kapral, G. J., Grosse-Kunstleve, R. W., McCoy, A. J., Moriarty, N. W., Oeffner, R., Read, R. J., Richardson, D. C., Richardson, J. S., Terwilliger, T. C., and Zwart, P. H. (2010) PHENIX. A comprehensive Python-based system for macromolecular structure solution. *Acta Crystallogr. D Biol. Crystallogr.* **66,** 213–221
16. Emsley, P., Lohkamp, B., Scott, W. G., and Cowtan, K. (2010) Features and development of Coot. *Acta Crystallogr. D Biol. Crystallogr.* **66,** 486–501
17. Clauser, K. R., Baker, P., and Burlingame, A. L. (1999) Role of accurate mass measurement (±10 ppm) in protein identification strategies employing MS or MS/MS and database searching. *Anal. Chem.* **71,** 2871–2882
18. Figueira, A. C., Saidemberg, D. M., Souza, P. C., Martínez, L., Scanlan, T. S., Baxter, J. D., Skaf, M. S., Palma, M. S., Webb, P., and Polikarpov, I. (2011) Analysis of agonist and antagonist effects on thyroid hormone receptor conformation by hydrogen/deuterium exchange. *Mol. Endocrinol.* **25,** 15–31

19. Gampe, R. T., Jr., Montana, V. G., Lambert, M. H., Miller, A. B., Bledsoe, R. K., Milburn, M. V., Kliewer, S. A., Willson, T. M., and Xu, H. E. (2000) Asymmetry in the PPARγ/RXRα crystal structure reveals the molecular basis of heterodimerization among nuclear receptors. *Mol. Cell* **5,** 545–555
20. Martínez, L., Andreani, R., and Martínez, J. M. (2007) Convergent algorithms for protein structural alignment. *BMC Bioinformatics* **8,** 306
21. Gordon, J. C., Myers, J. B., Folta, T., Shoja, V., Heath, L. S., and Onufriev, A. (2005) H++. A server for estimating pK_as and adding missing hydrogens to macromolecules. *Nucleic Acids Res.* **33,** W368–W371
22. Humphrey, W., Dalke, A., and Schulten, K. (1996) VMD: visual molecular dynamics. *J. Mol. Graph.* **14,** 33–38, 27–28
23. MacKerell, A. D., Bashford, D., Bellott, Dunbrack, R. L., Evanseck, J. D., Field, M. J., Fischer, S., Gao, J., Guo, H., Ha, S., Joseph-McCarthy, D., Kuchnir, L., Kuczera, K., Lau, F. T. K., Mattos, C., Michnick, S., Ngo, T., Nguyen, D. T., Prodhom, B., Reiher, W. E., Roux, B., Schlenkrich, M., Smith, J. C., Stote, R., Straub, J., Watanabe, M., Wiórkiewicz-Kuczera, J., Yin, D., and Karplus, M. (1998) All-atom empirical potential for molecular modeling and dynamics studies of proteins. *J. Phys. Chem. B* **102,** 3586–3616
24. Jorgensen, W. L., Chandrasekhar, J., Madura, J. D., Impey, R. W., and Klein, M. L. (1983) Comparison of simple potential functions for simulating liquid water. *J. Chem. Phys.* **79,** 926–935
25. Hansson, A., Souza, P. C. T., Silveira, R. L., Martínez, L., and Skaf, M. S. (2011) CHARMM force field parametrization of rosiglitazone. *Int. J. Quantum Chem.* **111,** 1346–1354
26. Leach, A. (2001) *Molecular Modeling: Principles and Applications*, 2nd Ed., Prentice Hall, Harlow, UK
27. Ryckaert, J., Ciccotti, G., and Berendsen, H. (1977) Numerical integration of the Cartesian equations of motion of a system with constraints. Molecular dynamics of *n*-alkanes *J. Comput. Phys.* **23,** 327–341
28. Phillips, J. C., Braun, R., Wang, W., Gumbart, J., Tajkhorshid, E., Villa, E., Chipot, C., Skeel, R. D., Kalé, L., and Schulten, K. (2005) Scalable molecular dynamics with NAMD. *J. Comput. Chem.* **26,** 1781–1802
29. Mourão, R. H., Silva, T. G., Soares, A. L., Vieira, E. S., Santos, J. N., Lima, M. C., Lima, V. L., Galdino, S. L., Barbe, J., and Pitta, I. R. (2005) Synthesis and biological activity of novel acridinylidene and benzylidene thiazolidinediones. *Eur. J. Med. Chem.* **40,** 1129–1133
30. Lu, M., Sarruf, D. A., Talukdar, S., Sharma, S., Li, P., Bandyopadhyay, G., Nalbandian, S., Fan, W., Gayen, J. R., Mahata, S. K., Webster, N. J., Schwartz, M. W., and Olefsky, J. M. (2011) Brain PPAR-γ promotes obesity and is required for the insulin-sensitizing effect of thiazolidinediones. *Nat. Med.* **17,** 618–622
31. Ryan, K. K., Li, B., Grayson, B. E., Matter, E. K., Woods, S. C., and Seeley, R. J. (2011) A role for central nervous system PPAR-γ in the regulation of energy balance. *Nat. Med.* **17,** 623–626
32. Zhang, H., Zhang, A., Kohan, D. E., Nelson, R. D., Gonzalez, F. J., and Yang, T. (2005) Collecting duct-specific deletion of peroxisome proliferator-activated receptor γ blocks thiazolidinedione-induced fluid retention. *Proc. Natl. Acad. Sci. U.S.A.* **102,** 9406–9411
33. Ohno, H., Shinoda, K., Spiegelman, B. M., and Kajimura, S. (2012) PPARγ agonists induce a white-to-brown fat conversion through stabilization of PRDM16 protein. *Cell Metab.* **15,** 395–404
34. Maier, C. S., and Deinzer, M. L. (2005) Protein conformations, interactions, and H/D exchange. *Methods Enzymol.* **402,** 312–360
35. Ali, A. A., Weinstein, R. S., Stewart, S. A., Parfitt, A. M., Manolagas, S. C., and Jilka, R. L. (2005) Rosiglitazone causes bone loss in mice by suppressing osteoblast differentiation and bone formation. *Endocrinology* **146,** 1226–1235
36. Yaturu, S., Bryant, B., and Jain, S. K. (2007) Thiazolidinedione treatment decreases bone mineral density in type 2 diabetic men. *Diabetes Care* **30,** 1574–1576
37. Schwartz, A. V., Sellmeyer, D. E., Vittinghoff, E., Palermo, L., Lecka-Czernik, B., Feingold, K. R., Strotmeyer, E. S., Resnick, H. E., Carbone, L., Beamer, B. A., Park, S. W., Lane, N. E., Harris, T. B., and Cummings, S. R. (2006) Thiazolidinedione use and bone loss in older diabetic adults. *J. Clin. Endocrinol. Metab.* **91,** 3349–3354
38. Olefsky, J. M. (2000) Treatment of insulin resistance with peroxisome proliferator-activated receptor γ agonists. *J. Clin. Invest.* **106,** 467–472
39. Choi, J. H., Banks, A. S., Kamenecka, T. M., Busby, S. A., Chalmers, M. J., Kumar, N., Kuruvilla, D. S., Shin, Y., He, Y., Bruning, J. B., Marciano, D. P., Cameron, M. D., Laznik, D., Jurczak, M. J., Schürer, S. C., Vidović, D., Shulman, G. I., Spiegelman, B. M., and Griffin, P. R. (2011) Antidiabetic actions of a non-agonist PPARγ ligand blocking Cdk5-mediated phosphorylation. *Nature* **477,** 477–481
40. Trujillo, M. E., and Scherer, P. E. (2006) Adipose tissue-derived factors. Impact on health and disease. *Endocr. Rev.* **27,** 762–778
41. Chandra, V., Huang, P., Hamuro, Y., Raghuram, S., Wang, Y., Burris, T. P., and Rastinejad, F. (2008) Structure of the intact PPAR-γ-RXR-nuclear receptor complex on DNA. *Nature* **456,** 350–356
42. Burgermeister, E. (2006) A novel partial agonist of peroxisome proliferator-activated receptor-γ (PPARγ) recruits PPARγ-coactivator-1α, prevents triglyceride accumulation, and potentiates insulin signaling *in vitro*. *Molecular Endocrinology* **20,** 809–830
43. Bruning, J. B., Chalmers, M. J., Prasad, S., Busby, S. A., Kamenecka, T. M., He, Y., Nettles, K. W., and Griffin, P. R. (2007) Partial agonists activate PPARγ using a helix 12-independent mechanism. *Structure* **15,** 1258–1271
44. Acton, J. J., 3rd, Black, R. M., Jones, A. B., Moller, D. E., Colwell, L., Doebber, T. W., Macnaul, K. L., Berger, J., and Wood, H. B. (2005) Benzoyl 2-methyl indoles as selective PPARγ modulators. *Bioorg. Med. Chem. Lett.* **15,** 357–362
45. Kim, J. Y., van de Wall, E., Laplante, M., Azzara, A., Trujillo, M. E., Hofmann, S. M., Schraw, T., Durand, J. L., Li, H., Li, G., Jelicks, L. A., Mehler, M. F., Hui, D. Y., Deshaies, Y., Shulman, G. I., Schwartz, G. J., and Scherer, P. E. (2007) Obesity-associated improvements in metabolic profile through expansion of adipose tissue. *J. Clin. Invest.* **117,** 2621–2637